Lattice symmetry of the cholesteric blue phases

S. Meiboom, M. Sammon, and D. W. Berreman
Bell Laboratories, Murray Hill, New Jersey 07974
(Received 16 May 1983)

The cholesteric blue phases (BP I and BP II) can be modeled as cubic lattices of disclinations in a cholesteric matrix. In an earlier paper we presented results of free-energy calculations for three models with O^2 ($P4_232$), O^5 ($I432$), and O^8 ($I4_132$) space-group symmetry. In the present paper calculations for a fourth model, also of O^8 symmetry, are presented (we differentiate these models as $O^{8(+)}$ and $O^{8(-)}$, respectively). For a number of cholesterol derivatives we assign the $O^{8(-)}$ structure to the BP I, and the O^2 structure to BP II, on the following evidence: For the case of equal elastic constants the calculations show a crossover of the free energy, the O^2 structure being lowest at the higher temperatures, and $O^{8(-)}$ at lower temperatures. (However, the crossover may disappear for other values of the elastic constants.) The assignment is consistent with the observed BP I and BP II lattice constants in terms of cholesteric pitch. There is excellent agreement between calculated and observed intensities of the Bragg reflections. Some details of the observed Bragg-diffraction spectra are also discussed.

I. INTRODUCTION

The cholesteric blue phases are stable in a narrow temperature range, of the order of 1 °C, immediately below the clearing point of cholesteric liquid crystals.[1] There has recently been a renewed interest in these phases, from the theoretical as well as the experimental aspects.[2–7] (These references will serve as a key to earlier work.) The present paper is a continuation of an earlier one,[8] in which we modeled the blue phases as a cubic lattice of disclinations. In this model the material between the cores of the disclinations is treated as uniaxial and characterized by the Oseen-Frank elasticity equations, and the reduction in free energy stabilizing the blue phases is ascribed to the establishment of double cholesteric twist. For a detailed discussion of the model we refer to the earlier paper.[8] In that paper we also presented results of computer calculations[9] of the free energy for three specific models, with O^2 ($P4_232$), O^5 ($I432$), and O^8 ($I4_132$) cubic symmetries. In what follows we shall make frequent references to these results, as well as to those in an earlier paper[7] reporting experimental results. Because it is impractical to reproduce here the many figures and graphs we shall refer to, a reader with more than a cursory interest should obtain copies of Refs. 7 and 8. For short, we shall refer to them as MS and MSB, respectively.

In the present paper we report free-energy computations for a new model with O^8 symmetry. In order to differentiate it from the earlier model of the same symmetry, we shall, for reasons which will become apparent below, designate it by $O^{8(-)}$, while the original, treated in MSB will be referred to as $O^{8(+)}$. We then discuss evidence for assigning specific symmetries to the experimentally observed blue phase I (BP I) and blue phase II (BP II) (blue phase III, or "blue fog," does not exhibit a periodic structure and will not be discussed here). The experimental results used in the assignment are those given in MS and apply to cholesteryl nonanoate and to mixtures of cholesteryl nonanoate and cholesteryl chloride. Though we believe these assignments may apply to many other systems which behave in a similar manner, we have no proof that this is indeed so.

Important evidence for specific assignments can come from a comparison of observed and calculated intensities of Bragg reflections. Optical structure factors for chiral cubic space groups have been derived by Hornreich and Shtrikman[10] but they do not give quantitative intensities. The latter have been calculated by Berreman[11] for our O^2, O^5, $O^{8(+)}$, and $O^{8(-)}$ models, using computer solutions of Maxwell's equations. We shall compare his results for the various models with observed intensities in cholesteryl esters. We conclude that, at least for the cholesterol derivatives referred to above, the blue phase I is body-centered cubic (bcc) with the $O^{8(-)}$ structure, while the blue phase II is simple cubic (sc), with the O^2 symmetry.

II. THE $O^{8(-)}$ STRUCTURE

A cubic structure with O^8 symmetry was first proposed by Hornreich and Shtrikman.[12] As described in MSB, we set up a director model by first constructing a tensor model of the required symmetry. Following Alexander[13] and Grebel, Hornreich, and Shtrikman[3] this model is obtained by superposing a suitable set of order parameter waves, as follows:

$$Q_{\alpha\beta}(\vec{r}) \equiv \sum_n Q^n_{\alpha\beta} e^{i\vec{q}_n\cdot\vec{r}} ,$$

where the $\vec{q}_n$ are a set of reciprocal-lattice vectors, and the $Q^n_{\alpha\beta}$ are determined by the symmetry group of the lattice being studied. Expressions for the $Q_{\alpha\beta}(\vec{r})$ for the various lattice symmetries can be found in Refs. 3, 9, or 11. The director, $\vec{n}(\vec{r})$, is obtained by diagonalizing $Q_{\alpha\beta}(\vec{r})$ and choosing $\vec{n}(\vec{r})$ to be the eigenfunction giving the maximum positive (prolate) eigenvalue. This procedure is well defined, except on lines where there are two

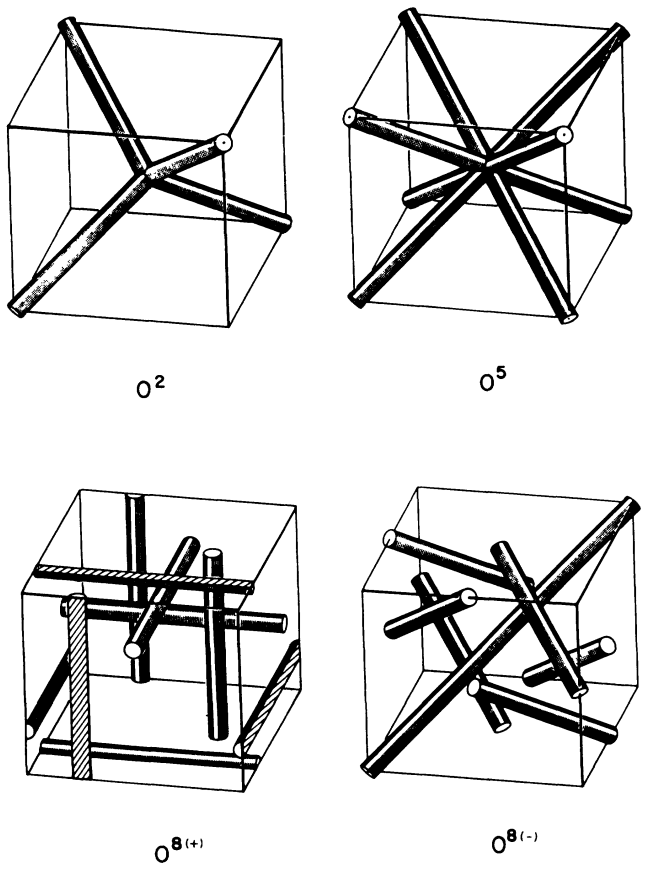

FIG. 1. Configuration of the disclinations in the cubic unit cells of the various models.

degenerate maximum eigenvalues. As argued in MSB, these lines correspond to the $s=-\frac{1}{2}$ disclinations of the director model.

The process of diagonalization of the tensor and localization of the disclinations is done numerically for a three-dimensional mesh in the unit cell. The $O^{8(-)}$ symmetry is obtained by replacing $Q_{\alpha\beta}(\vec{r})$ for the $O^{8(+)}$ by its negative value. That is, we interchange the positions of the disclinations (i.e., oblate order tensors) and double twist tubes[8] (i.e., prolate order tensors). The disclination configurations for the various structures are given in Fig. 1. Note that this procedure for obtaining a new structure cannot be applied to the O^2 and O^5 symmetries. In the latter structures the order tensor has singular points (the center and corners of the unit cell), and does not define a director at these points.

As described in MSB and Ref. 9, the director configuration is put through a number of numerical relaxation cycles, so as to minimize the Oseen-Frank free energy. The results of the free-energy computations for the $O^{8(-)}$ structure are plotted in Figs. 2 and 3, for the cases of equal elastic constants ($K_{11}=K_{22}=K_{33}$) and for unequal ones ($K_{11}=2K_{22}=K_{33}$), respectively. These figures will be compared with the corresponding ones for the O^2, O^5, and $O^{8(+)}$ symmetries given in MSB.

The director configurations for the various symmetries were used in a numerical computation of the relative intensities of the first few Bragg reflections. Details of the procedure are given by Berreman.[11] The results are summarized in Table I. The calculated intensities given there were actually computed for the case $K_{11}=2K_{22}=K_{33}$. However, the case $K_{11}=K_{22}=K_{33}$ produces the same

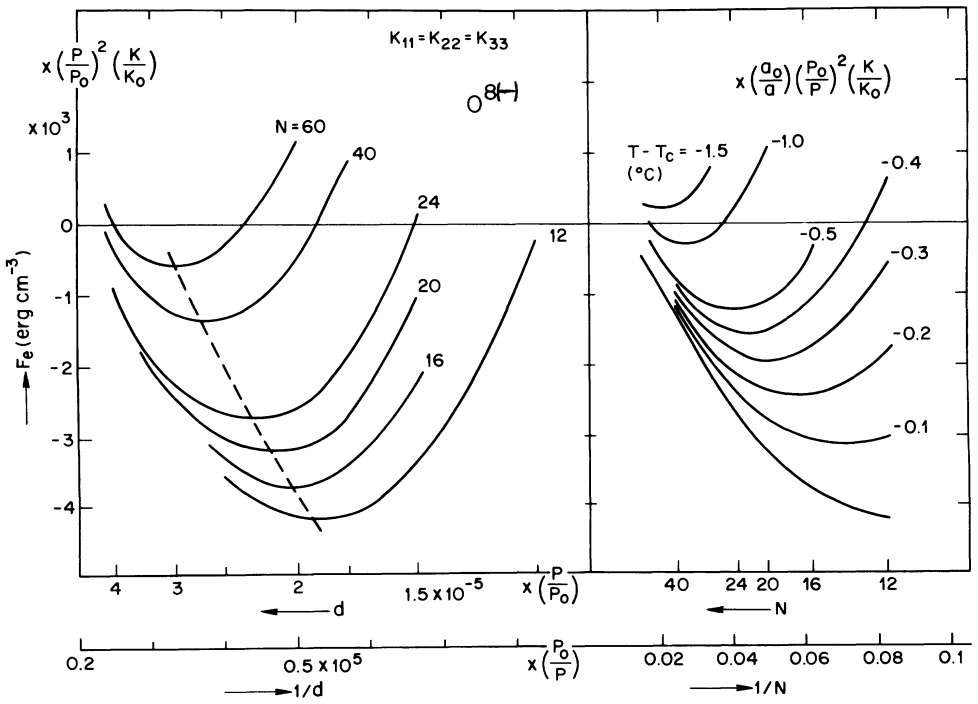

FIG. 2. Free-energy curves for the $O^{8(-)}$ structure for the case of equal elastic constants. These curves are comparable to those for other symmetries given in Figs. 5—10 of MSB (Ref. 8). We refer to that article for methods of calculation and parameters used.

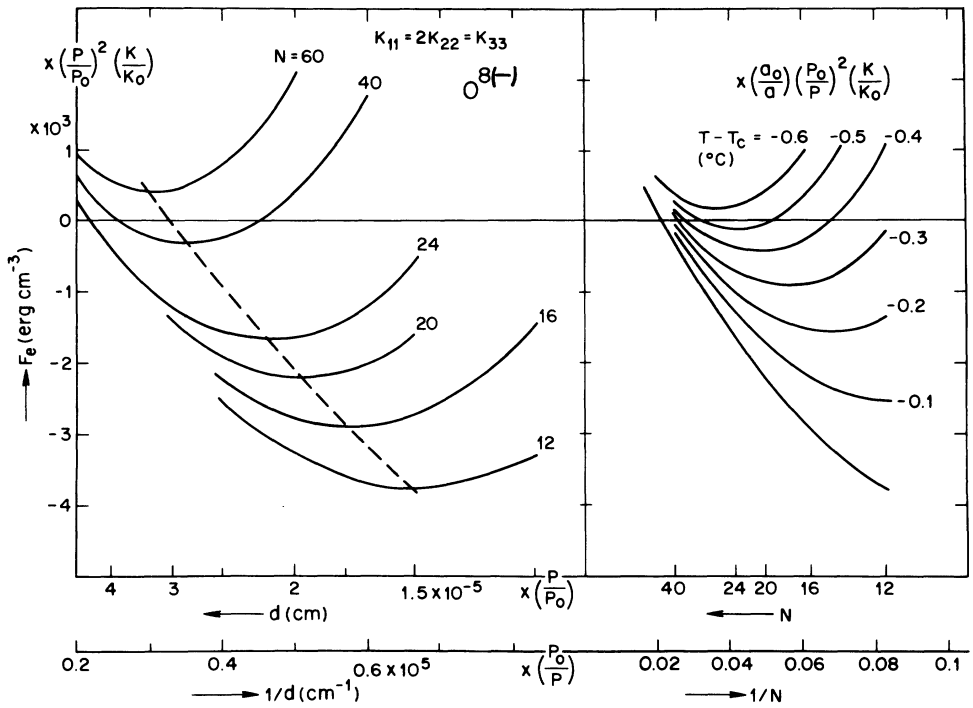

FIG. 3. Free-energy curves for the $O^{8(-)}$ structure for the case $K_{11}=2K_{22}=K_{33}$. Other details as for Fig. 2.

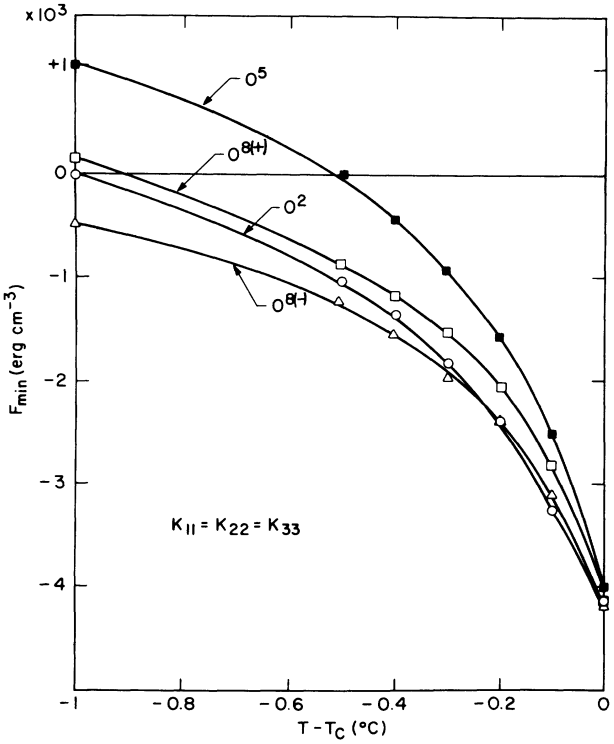

FIG. 4. Calculated minimum free energy for the various structures as function of temperature (T) relative to the clearing point (T_c). The zero of the free-energy scale corresponds to the free energy of the ordinary (helical) cholesteric. The graphs are for the case of equal elastic constants.

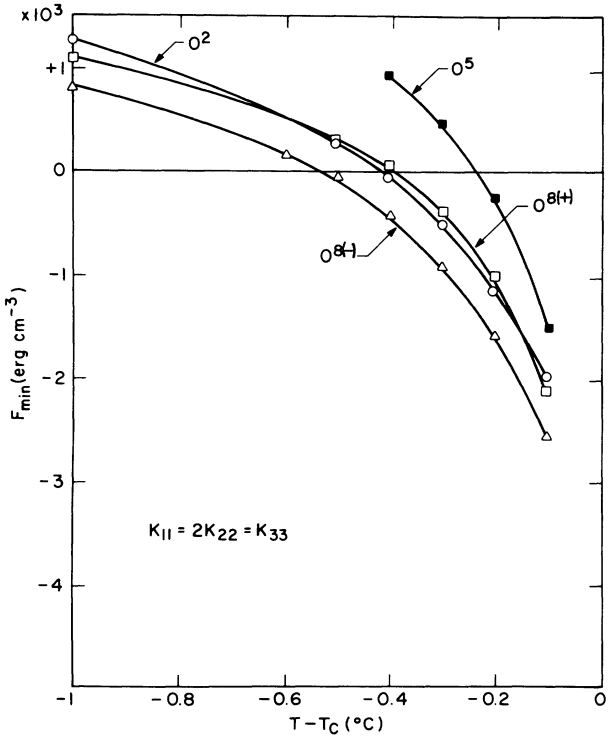

FIG. 5. Same as Fig. 4, but for the case $K_{11}=2K_{22}=K_{33}$.

TABLE I. Comparison of calculated and observed relative intensities of Bragg reflections.

Reflection number	Miller indices sc O^2	Miller indices bcc O^5, O^8	Relative intensities[a] Observed[b] BP I	Observed[b] BP II	Calculated[c] O^2	Calculated[c] O^5	Calculated[c] $O^{8(+)}$	Calculated[c] $O^{8(-)}$
1	100	110	(1)	(1)	(1)	(1)	(1)	(1)
2	110	200	0.54	0.29	0.30	0	0.01	0.53
3	111	211	0.20	<0.05	0	0	0.13	0.22
4	200	220	<0.05	<0.05	0	0.05	0	0

[a]Intensities are normalized to give unity for the first reflection. Zeros for the calculated intensities indicate values smaller than 0.001.

[b]Observed intensities apply to cholesterol derivatives, and were obtained from the magnitudes of the steps in the spectra of Fig. 4 of MS (Ref. 7) and a number of similar spectra, including some of longer pitch material (cholesteryl nonanoate with up to 30% chloride). Some details of the procedure are given in Ref. 18.

[c]From Ref. 11.

values within the precision given. A comparison of the calculated intensities with the observed ones will be discussed in the next section.

III. SYMMETRY ASSIGNMENTS

In this section we shall present evidence for the assignment of specific symmetries to the BP I and BP II phase.

A. Theoretical predictions

The results of the computer calculations for the various models are summarized in Fig. 4 for the case $K_{11}=K_{22}=K_{33}$, and in Fig. 5 for the case $K_{11}=2K_{22}=K_{33}$. The curves give the calculated free energy as function of the temperature and were obtained from Figs. 2 and 3 for the $O^{8(-)}$ model, and from Figs. 5–10 of MSB for the O^2, O^5, and $O^{8(+)}$ models. We simply plotted the free energy at the minima of the curves in the right-hand part of these figures, as function of the $T-T_c$ (i.e., the temperature relative to the clearing point). In a few cases the minima are just outside the plotted range, and were obtained by extrapolation. Note that on the energy scale used the helical cholesteric has zero free energy.

Referring to Fig. 4 for the case $K_{11}=K_{22}=K_{33}$, it is seen that the curves for O^2 and $O^{8(-)}$ cross, the former being the stable structure at the higher temperatures, and the latter at the lower temperatures (at still lower temperatures the helical cholesteric becomes stable). It is therefore suggestive to identify the BP I with the $O^{8(-)}$ structure. However, for the case $K_{11}=2K_{22}=K_{33}$, given in Fig. 5, the $O^{8(-)}$ has the lowest free energy up to the clearing point, and no BP I to BP II transition is predicted. Note that for our simple model (and neglecting surface terms) the relative stability of the various symmetries (that is the relative vertical position of the curves in Figs. 4 and 5), depends only on the ratios of the elastic constants. As discussed in some detail in MSB, changes in the cholesteric pitch, in the absolute values of the elastic constants (while leaving their ratios constant), and in the enthalpy of transition introduce scale factors for the free energy, for the unit cell dimension, and for the temperature, but otherwise leave the curves unaltered. We have found no experimental values for the elastic constants for cholesterol derivatives in the literature, no doubt because their helicity makes measurements difficult. In nematics,

TABLE II. Comparison of calculated and observed wavelengths of the lowest-order Bragg reflection. The wavelengths are given relative to that of the helical cholesteric, taken as unity.

	Lattice constant (nm) Calculated[a] $K_{11}=K_{22}=K_{33}$	Lattice constant (nm) Calculated[a] $K_{11}=2K_{22}=K_{33}$	Wavelength ratios Calculated[b] $K_{11}=K_{22}=K_{33}$	Wavelength ratios Calculated[b] $K_{11}=2K_{22}=K_{33}$	Observed[c] CH	Observed[c] BP
Cholesteric	125	125	(1)	(1)	(1)	(1)
O^2	147	154	1.18	1.23		
O^5	213	238	1.20	1.35		
$O^{8(+)}$	213	213	1.20	1.20		
$O^{8(-)}$	238	222	1.35	1.26		
BP I					1.27	1.40
BP II					1.10	1.24

[a]Calculated values from Figs. 2 and 3 of the present paper, and from Figs. 5–10 of MSB. For the helical cholesteric the repeat distance is one-half of the pitch of 250 nm assumed in the calculations.

[b]Ratios of the values in the first two columns, allowing for a factor of $1/\sqrt{2}$ for the bcc (O^5 and O^8) (see text).

[c]Observed wavelength ratios of the lowest-order Bragg reflections for cholesterol derivatives (CH) and for a mixture of biphenyl compounds (BP), from Refs. 7 and 14 and 15, respectively.

K_{22} tends to be appreciably smaller than K_{11} and K_{33}. This, however, may not apply to the cholesterol derivatives, which are structurally very different from the nematics. Obviously, the differences in calculated free energy of the various models are quite small, and sensitive to changes in parameters. This, and the fact that our models are hardly rigorous, makes it hard to argue that the above assignment of BP I to $O^{8(-)}$ and BI II to O^2 is more than a coincidence. However, there is other evidence in support of this assignment, and we shall proceed by comparing its consequences with experiment.

B. Wavelengths of the Bragg reflections

An important check on the theory is provided by a comparison of the calculated lattice constants of the blue phase for a specific cholesteric pitch with those observed experimentally. As the lattice constants determine the wavelengths of the Bragg reflections, we compare calculated and observed wavelengths of the lowest-order Bragg reflections in the ordinary (helical) cholesteric and in the BP I and BP II phases. In Table II are given ratios of the wavelength of the lowest-order Bragg reflection in the blue phases to the wavelength of the Bragg reflection in helical cholesteric. (This ratio for the helical cholesteric is thus unity by definition, as indicated in Table II.)

Some comments as to how Table II was arrived at are in order. The calculated lattice constants for the various models were obtained from Figs. 2 and 3 of the present paper for the $O^{8(-)}$, and from Figs. 5–10 of MSB for the other models. The construction for obtaining the lattice constant from the figure is indicated in Fig. 7 of MSB. We have assumed a temperature $T-T_c$ of $-0.2\,^{\circ}\mathrm{C}$, which should be near the BP I to BP II transition. The repeat distance for the Bragg reflection in the helical cholesteric is one-half the pitch of 250 nm assumed in the calculations. The calculated wavelength ratios in Table II are simply the ratios of the corresponding lattice constants, except that a factor of $1/\sqrt{2}$ must be introduced for the bcc lattices (O^5 and O^8). This is because the lowest-order nonzero Bragg reflection in bcc is 110 rather than 100. As a result of the scaling mentioned in the preceding section, the wavelength ratios should be largely independent of the actual values of the parameters, except for the ratios of the elastic constants and for the scaling of the temperature. In respect to the latter, it can be shown that its effect on the ratios is minimal for any reasonable values of the parameters.

The observed wavelength ratios given in Table II for comparison with the calculated ones are for cholesterol derivatives (indicated by CH) and for a biphenyl mixture (indicated by BP). The CH numbers are taken from Fig. 7 of MS, which applies to cholesteryl nonanoate, and from Figs. 4 and 5 of MS, which apply to a mixture of 85% cholesteryl nonanoate and 15% cholesteryl chloride. The observed wavelengths for the helical cholesteric, the BP I and the BP II are, respectively, 360, 445, and 395 nm for the nonanoate, and 445, 575, and 490 nm for the mixture. (The wavelengths for the BP I and BP II are somewhat temperature dependent, and were taken near the transition between these two phases, i.e., about 0.2 °C below the clearing point.) The ratios of the above wavelengths are 1:1.24:1.10 and 1:1.29:1.10, respectively, for an average of 1:1.27:1.10. The BP numbers in Table II are taken from Johnson *et al.*[14] and Her *et al.*,[15] and apply to a 50-50 vol % mixture of CB15 and E9 biphenyls.[16] Both papers give essentially the same ratio of 1:1.40:1.24 given in Table II. (The reality of the BP IIB phase discussed in the papers is in doubt.[17])

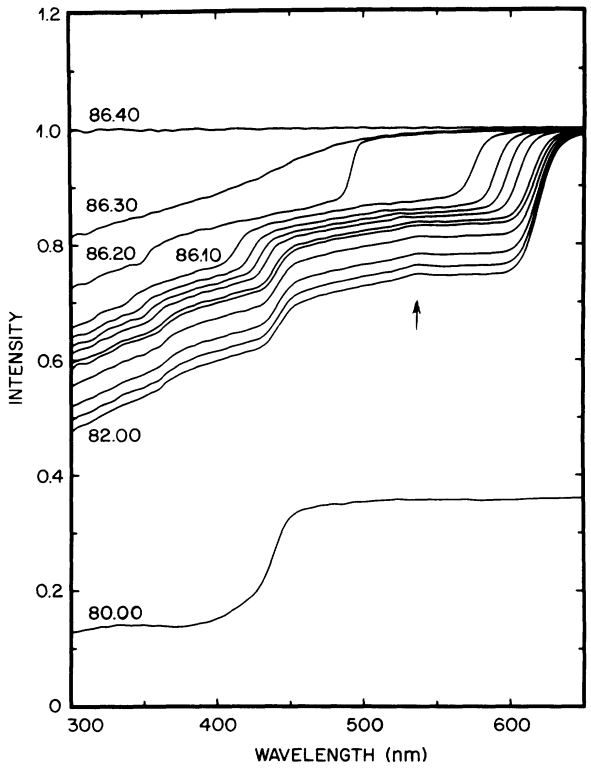

FIG. 6. Transmission spectra of a mixture of 85% cholesteryl nonanoate and 15% cholesteryl chloride (by weight). The sample cell had been cleaned by a plasma discharge in O_2, producing a powder spectrum. Traces were recorded in order of decreasing temperature. Where not indicated in the figure, the temperatures, from top to bottom, are (in °C) 86.00, 85.90, 85.80, 85.60, 85.50, 85.00, 84.00, 83.00. From MS (Ref. 7).

What conclusions can be drawn from Table II? First, the calculated wavelength ratios do not vary much from model to model, and are of similar magnitude as the observed ones. One can consider this as a semiquantitative confirmation for the kind of model treated here. However, because the variation of the ratios with model is slight, and of the same magnitude as their variation with elastic constants, it seems unwarranted to draw general conclusions as to specific symmetries. For the cholesterol derivatives an assignment of O^2 to BP II and $O^{8(-)}$ to BP I gives the best fit of observed and calculated values for the case of equal elastic constants, but not for the case of unequal constants. The assignment, though suggestive, is thus hardly convincing.

C. Intensities of the Bragg reflections

The best evidence for specific symmetries for the blue phases comes from a comparison of observed and calcu-

lated intensities of the Bragg reflections. The relevant data are given in Table I. The last four columns give the intensities calculated by Berreman,[11] normalized to unity for the lowest-order reflection. The observed relative intensities apply to cholesterol derivatives, and were obtained from the magnitudes of the steps in powder spectra such as Fig. 4 of MS, which is reproduced here as Fig. 6. (Spectra of oriented samples, like Fig. 6 of MS, are not suited for this purpose, because the distribution of crystallite orientations is unknown. In the powder spectra the absence of any noticeable dips attests to an isotropic distribution.) In order to convert step magnitudes into scattering intensities, the establishment of a spectrum baseline is necessary. Because only one circularly polarized component is Bragg scattered, the baseline is at some finite intensity value, rather than at the zero-intensity axis. Details of the procedure adopted in establishing the baseline are given in Ref. 18.

A perusal of Table I produces assignments of $O^{8(-)}$ to the BP I, and of O^2 to BP II. In fact, the agreement is almost embarrassingly good, and considering the uncertainties in both calculations and observations, must to some degree be ascribed to chance. However, even if some latitude is allowed, any alternative assignment among the models listed is clearly ruled out.

D. Various spectrum features

In this section we discuss a number of features in the spectra of the blue phases which may give additional information about their structure. One small, but consistent, feature appears in the powder spectra of the BP I. It is seen in Fig. 6 as the small upward blip pointed at by the arrow. Its position on the lower traces of the figure is at about 535 nm, while the lowest-order Bragg step is at 615 nm. The ratio of these two numbers is, within accuracy, $(\frac{3}{4})^{1/2}$. Though weak, the consistency of the feature for different temperatures and for samples of different pitch, and the fact that it always appears at the same $(\frac{3}{4})^{1/2}$ position, attest to its reality. We advance the following, somewhat tentative, interpretation, based on the dynamical theory of x-ray scattering (which, suitably adapted, should, of course, apply here). This theory predicts a reduction of intensity of a Bragg reflection (and thus an increase in transmission), whenever the crystal orientation is such that the Bragg condition is simultaneously satisfied for two sets of crystal planes. This effect is sometimes referred to as the "brightening" effect ("Aufhellung"), and a detailed discussion is given by Pinsker.[19] In a bcc structure the longest wavelength for which the Bragg condition can be satisfied simultaneously for two sets of planes occurs for the (110) and (011) planes (or equivalent pairs). For a simultaneous reflection to occur the incident ray much bisect these two planes, and it is easily shown[20] that the smallest value of the sine factor in the Bragg condition is $(\frac{3}{4})^{1/2}$, in accordance with the observed position. It should, however, be pointed out that according to this simple argument simultaneous reflection would occur for all incident beam directions contained within the plane bisecting the crystallographic planes involved (oblique incidence), and not only for that direction coplanar with the normals to the planes (normal incidence). Thus in a powder spectrum one would expect an upward step in the spectrum, rather than the narrow upward blip observed. However, the actual situation is more complex, and it can, for instance, be argued that in the present case one must decompose the incident beam into circularly polarized components, which interact differently with the two crystallographic planes when the incidence is oblique (the geometries of the two reflections are mirror images). Only for normal incidence are the two reflections truly equivalent. A rigorous treatment of dynamical scattering for three waves applicable to the present case will be very complex, and we have not attempted it.

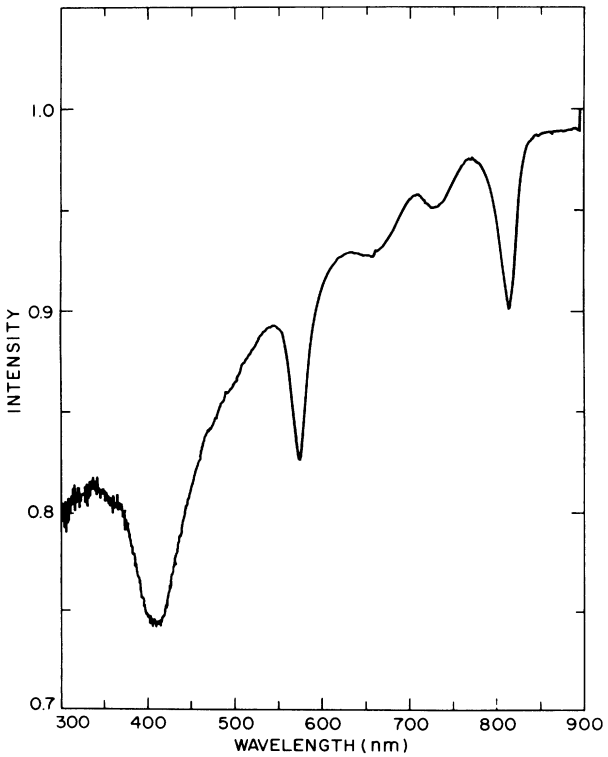

FIG. 7. Transmission spectrum of a mixture of 75% cholesteryl nonanoate and 25% cholesteryl chloride (by weight). The sample cell was 0.3 mm thick and the inside surface was treated with polyimide and rubbed.

In the case of simple cubic structures, the longest wavelength for two simultaneous Bragg reflections is for the {100} planes. These planes are orthogonal in pairs, and thus the minimum angle of incidence for simultaneous reflection is 45° and the corresponding wavelength $1/\sqrt{2}$ of that of the lowest-order reflection. As this position would coincide with the much stronger (110) step, it could not be observed. In fact, we have never observed the blip in the BP I spectrum. Thus if our interpretation is correct, it is strong evidence for bcc symmetry of the BP I.

A different feature appears in oriented samples (obtained by treating the surfaces of the cell with surfactant). It consists of additional dips that do not correspond to steps in the powder spectra. Examples are given in Fig. 7 and in Figs. 2, 3, 6, and 7 of MS. It seems natural to ascribe these dips to crystallites preferentially oriented on

the surface of the cell. Whether, and at what wavelengths, dips appear depends on the surface preparation, which for instance is different in the sample of Fig. 7 and those in Figs. 2, 3, 6, and 7 of MS. Also, the additional dips tend to weaken, and sometimes totally disappear, as the sample ages over a few days, indicating a process of recrystallization.

Some of the dips allow a simple interpretation. The one at 660 nm in Fig. 7 is at a wavelength very nearly $(\frac{2}{3})^{1/2}$ times the wavelength of the lowest order dip (814 nm). For a bcc structure this ratio applies to the 110 reflection in crystallites oriented with their (111) planes parallel to the cell wall[21] (note that the 111 reflection is absent in bcc, and thus no step is expected in the powder spectrum). For a sc structure the same dip could correspond to a 100 reflection in (211) oriented crystallites. Dips with the same relative position of $(\frac{2}{3})^{1/2}$ also appear in Figs. 2, 3, 6, and 7 of MS. Note that the additional dips under discussion are in general broader than the normal dips. This is as expected: the latter are caused by back reflection, and any misalignment of the crystallites affects the Bragg reflection wavelength only to second order. The additional dips involve reflection through a finite angle, and a misalignment enters in first order.

Some other characteristics of the spectra remain mysterious. We have been unable to find a plausible explanation for the dip at 730 nm in the spectrum of Fig. 7. No crystallite orientation with reasonably small Miller indices will do, either for bcc or for sc. Similarly, the dip at about 370 nm in Figs. 2 and 3 of MS remains a puzzle. It cannot be the {211} back reflection in bcc, which would be at this position, because the {110} reflection from the same crystallites should be easily observable, and is not evident. In sc the {100} reflection from ⟨111⟩ oriented crystallites would appear at this position, but all other evidence contradicts a sc structure for the BP I. (For instance, in any sc structure the {111} reflection should be absent,[10] while it clearly appears in the powder spectra.)

We have not been able to elucidate these points. As the BP I is reached by cooling from the BP II phase (heating from the cholesteric does not produce well-aligned samples), one can speculate that the oddly oriented BP I crystallites are remainders of the BP II to BP I transition. Under the microscope one can indeed see that there is a memory of the BP II pattern after transformation to BP I. But this is an *ad hoc* explanation at best.

IV. DISCUSSION

From the foregoing we conclude that the BP I and BP II have the $O^{8(-)}$ and O^2 structures, respectively. It should be stated that we believe this to apply to a range of cholesterol derivatives we have studied, including butyrate, valerate, nonanoate, myristate, and a number of mixtures of nonanoate and chloride. All these compounds exhibit both BP I and BP II phases, and their spectra are essentially identical, provided the wavelength is scaled in proportion to the cholesteric pitch. We have not studied other classes of cholesteric compounds ("chiral nematics"). Although data in the literature[14,15,17] indicate a similar behavior for biphenyl mixtures, no powder spectra (and thus no relative intensities for the Bragg reflections) are available. It is therefore unclear whether the above assignments apply to these compounds too.

We now compare our results with relevant ones in the literature. Marcus[22] has concluded from morphological evidence that BP II is sc, while BP I is probably bcc. Onusseit and Stegemeyer[23] similarly conclude that BP II is sc, while BP I could be either sc or bcc. More specific assignments have been given by Flack *et al.*,[4] based on the Bragg scattering selection rules derived by Hornreich and Shtrikman[10] and their own observations of the presence or absence of specific reflections. They assign O^8 to BP I and either O^2 or O^8 to BP II. On the other hand, Nicastro and Keyes,[6] using the same selection rules, assign an O^5 structure to the BP I in the cholesteryl alkanoates with chain lengths 5, 6, 7, and 9 (valerate, hexanoate, heptanoate, and nonanoate). They observe these compounds in back reflection, and find the second reflection (at $1/\sqrt{2}$ of the longest wavelength one) to be absent. This observation is the principal basis for their O^5 assignment. The fact that a second reflection is seen in Figs. 6 and 7 of MS is explained away by the above authors by ascribing it to the {110} reflection from ⟨100⟩ oriented platelets. However, the second reflection is also observed as a step in powder spectra, as in Fig. 4 of MS, and here must be due to the {200} reflection (for the bcc case). We must add that, though Fig. 4 of MS is for a mixture of cholesteryl nonanoate and cholesteryl chloride, we observe the same reflections (shifted to shorter wavelengths) in pure nonanoate (unpublished spectra). In fact, we have observed the corresponding reflections in all cholesteryl derivatives we looked at, including butyrate, valerate, nonanoate, and myristate. We must conclude that the O^5 assignment is inconsistent with our data.

Summarizing, we believe that the experimental evidence points to the assignment of the bcc $O^{8(-)}$ structure to the BP I, and of the sc O^2 structure to the BP II, at least in the cholesterol derivatives we investigated, (cholesteryl valerate, butyrate, nonanoate, myristate, and mixtures of nonanoate and chloride). It is of course quite possible that other compounds will exhibit different structures. Theory indicates that such variability may be due to variations in elastic constants.

Finally, there is the question whether, within the framework of chiral cubic space groups, structures other than the ones discussed (O^2, O^5, $O^{8(+)}$, and $O^{8(-)}$) are possible. In particular, can two or more different structures exist with the same space group symmetry, as exemplified by the $O^{8(+)}$ and $O^{8(-)}$ structures? We have as yet no answer to this question.

[1]A. Saupe, Mol. Cryst. Liq. Cryst. 7, 59 (1969).

[2]S. A. Brazovskii and S. G. Dmitriev, Zh. Eksp. Teor. Fiz. 69, 979 (1975) [Sov. Phys.—JETP 42, 497 (1976)]; S. A. Brazovskii and V. M. Filev, *ibid.* 75, 1140 (1978) [48, 573 (1978)].

[3]H. Grebel, R. M. Hornreich, and S. Shtrikman, Phys. Rev. A 28, 1114 (1983).

[4]J. H. Flack, P. P. Crooker, and R. C. Svoboda, Phys. Rev. A 26, 723 (1982).

[5]H. Onusseit and H. Stegemeyer, Chem. Phys. Lett. 89, 95 (1982).

[6]A. J. Nicastro and P. H. Keyes, Phys. Rev. A 27, 431 (1983).

[7]S. Meiboom and M. Sammon, Phys. Rev. A 24, 468 (1981). Referred to as MS.

[8]S. Meiboom, M. Sammon, and W. F. Brinkman, Phys. Rev. A 27, 438 (1983). Referred to as MSB.

[9]M. J. Sammon, Mol. Cryst. Liq. Cryst. 89, 305 (1982).

[10]R. M. Hornreich and S. Shtrikman, Phys. Lett. 82A, 354 (1981).

[11]D. W. Berreman, in *Liquid Crystals and Ordered Fluids,* Proceedings of an Am. Chem. Soc. Symposium, Las Vegas, 1982 (Plenum, New York, 1983), in press), Vol. 4.

[12]R. M. Hornreich and S. Shtrikman, Phys. Lett. 84A, 20 (1981).

[13]S. Alexander, in *Symmetries and Broken Symmetries in Condensed Matter Physics, Proceedings of the Colloque Pierre Curie, 1980,* edited by N. Boccara (Institut pour le Développement de la Science, l'Education et la Technologie, Paris, 1981).

[14]D. L. Johnson, J. H. Flack, and P. P. Crooker, Phys. Rev. Lett. 45, 641 (1980).

[15]J. Her, B. B. Rao, and J. T. Ho, Phys. Rev. A 24, 3272 (1981). Note that some plots in this paper are for higher-order Bragg reflections.

[16]These are British Drug House designations for their biphenyl derivatives. CB15 is an abbreviation for 4-cyano-4′-(2-methyl)butylbiphenyl.

[17]M. A. Marcus, Mol. Cryst. Liq. Cryst. 82, 33 (1982).

[18]The spectra of Fig. 4 of MS were made with unpolarized light, and essentially one circularly polarized component is Bragg scattered, while the other component is not. This would imply a horizontal baseline at 0.5 on the intensity axis. In fact, there appears to be some additional scattering and depolarization at the shorter wavelengths (probably due to grain boundaries and other imperfections). We account for this by adopting a baseline that starts at 0.5 at the longest wavelength, and continues parallel to the BP I curves, except that the steps in the latter are ignored. (In other words, the baseline has the same slope as the original spectrum between steps.) The resulting baseline goes smoothly from 0.5 at the right side of the figure to about 0.33 at the left side. Justification for this procedure can be found in the fact that nearly the same baseline is obtained from the higher-temperature BP I spectra as from the lower-temperature ones, even though the Bragg scattering intensity differs by nearly a factor of 2. Also, a similar scattering is observed for the non-Bragg scattered circularly polarized component, as given in Fig. 11 of MS. It can be noted that the observed scattering intensities, as given in Table I, are not very sensitive to the exact position of the baseline.

[19]Z. G. Pinsker, *Dynamical Scattering of X-Rays in Crystals* (Springer, New York, 1978), Chap. 12.

[20]In the cubic system the Miller indices of a plane can be taken as the components of a vector normal to it. The angle α between two planes with indices (abc) and (pqr), is given by the dot product of their normals: $\cos\alpha=(ap+bq+cr)/[(a^2+b^2+c^2)(p^2+q^2+r^2)]^{1/2}$. The angle θ between the incident beam and a plane (the sine of which appears in the Bragg condition) is $90°-\alpha/2$. For the case of planes (110) and (011) this becomes $\cos\alpha=0.5$, $\sin\theta=\cos(\frac{1}{2}\cos^{-1}0.5)=(\frac{3}{4})^{1/2}$.

[21]A derivation similar to the one in Ref. 20 gives for the ratio of the wavelength of the *abc* reflection in a (pqr) oriented crystallite and the wavelength of the 100 back reflection, $R=(ap+bq+cr)/[(a^2+b^2+c^2)(p^2+q^2+r^2)^{1/2}]$. As written this equation applies to sc. In bcc the lowest-order reflection is $\{110\}$, and if the ratio is referred to it, a factor $\sqrt{2}$ must be multiplied into the above equation.

[22]M. Marcus, Phys. Rev. A 25, 2272 (1982).

[23]H. Onusseit and H. Stegemeyer, Z. Naturforsch. Teil A 36, 1083 (1981).